JACS
JOURNAL OF THE AMERICAN CHEMICAL SOCIETY

ARTICLE

pubs.acs.org/JACS

Guanine-Rich RNAs and DNAs That Bind Heme Robustly Catalyze Oxygen Transfer Reactions

Lester C.-H. Poon,[†] Stephen P. Methot,[†] William Morabi-Pazooki,[†] Frédéric Pio,[†] Andrew J. Bennet,[‡] and Dipankar Sen[†,‡,*]

[†]Department of Molecular Biology & Biochemistry and [‡]Department of Chemistry, Simon Fraser University, Burnaby, British Columbia V5A 1S6, Canada

Supporting Information

ABSTRACT: Diverse guanine-rich RNAs and DNAs that fold to form guanine quadruplexes are known to form tight complexes with Fe(III) heme. We show here that a wide variety of such complexes robustly catalyze two-electron oxidations, transferring oxygen from hydrogen peroxide to thioanisole, indole, and styrene substrates. Use of ^{18}O-labeled hydrogen peroxide reveals the source of the oxygen transferred to form thioanisole sulfoxide and styrene oxide to be the activated ferryl moiety within these systems. Hammett analysis of the kinetics of thioanisole sulfoxide formation is unable to distinguish between a one-step, direct oxygen transfer and a two-step, oxygen rebound mechanism for this catalysis. Oxygen transfer to indole produces a range of products, including indigo and related dyes. Docking of heme onto a high-resolution structure of the G-quadruplex fold of Bcl-2 promoter DNA, which both binds heme and transfers oxygen, suggests a relatively open active site for this class of ribozymes and deoxyribozymes. That heme-dependent catalysis of oxygen transfer is a property of many RNAs and DNAs has ramifications for primordial evolution, enzyme design, cellular oxidative disease, and anticancer therapeutics.

INTRODUCTION

The broad-ranging catalytic possibilities of both RNA and DNA have been recognized in the past few decades. Nature offers several examples of RNA enzymes (ribozymes),[1] while functionally analogous catalytic DNAs (DNAzymes) have been artificially evolved in laboratories.[2] The catalytic repertoire of the nucleic acids is central to the concept of a primordial "RNA world",[3−5] in which primitive cells incorporating RNAs capable of self-replication and metabolic catalysis may have preceded contemporary protein- and nucleic acid-based organisms. The RNA world hypothesis has provided a major impetus for discovering new catalytic activities for the nucleic acids.[6] RNA and DNA are functionality poor compared to proteins; therefore, primordial ribozymes may have used cofactors to offset this chemical limitation, just as many contemporary proteins do to augment their own chemical repertoires.[4]

Heme is a ubiquitous metabolic cofactor and participates in a diversity of cellular functions, including electron transfer, the transport and sensing of diatomic gases, and various kinds of oxidative catalysis. Heme enzymes catalyzing oxidative reactions include the peroxidases and the P450 monooxygenases. A functional continuum exists between these enzymes: "classical" peroxidases, such as horseradish peroxidase (HRP), primarily catalyze 1-electron oxidations,[7,8] whereas "nonclassical" peroxidases, such as chloroperoxidase (CPO), display an intermediate function between classical peroxidases and P450 monooxygenases. The P450 enzymes, activated by dioxygen [or hydrogen peroxide (H_2O_2) in vitro], catalyze 2-electron oxidations characterized by oxygen atom transfer to the substrate. The heme cofactors in all of these enzymes are activated to an oxoiron species called compound I (Figure 1), in which the iron has a formal oxidation state of +5, although the dominant resonance contributor is thought to have the iron as Fe^{4+}, with the remaining oxidizing equivalent localized either on the porphyrin or on an amino acid side chain of the apoprotein.[7,8] For the heme enzymes that catalyze 2-electron oxidations, two contrasting mechanisms have been proposed: a direct transfer of oxygen from compound I to the substrate[7] and two successive 1-electron oxidations that proceed via a substrate radical intermediate[6] (Figure 1). The latter mechanism, called "oxygen rebound", is thought to operate in most heme enzymes.[7,8]

We have reported an 18-nucleotide DNAzyme, PS2.M, that binds Fe(III) heme and catalyzes 1-electron peroxidation reactions.[9] PS2.M was in vitro selected from a single-stranded, random-sequence, DNA library for its ability to bind *N*-methylmesoporphyrin IX (NMM), a transition-state analogue for porphyrin metalation.[10] PS2.M's catalysis of porphyrin metalation[10] was inhibited by Fe(III) heme, which itself bound to PS2.

Received: September 22, 2010

dx.doi.org/10.1021/ja108571a | *J. Am. Chem. Soc.* XXXX, XXX, 000–000

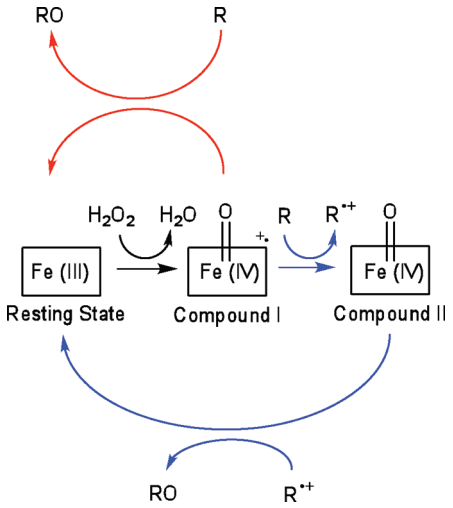

Figure 1. Alternative mechanisms for 2-electron oxidations catalyzed by heme enzymes. Blue arrows depict the two-step, oxygen-rebound mechanism, while the red arrow depicts a one-step, direct oxygen transfer mechanism.

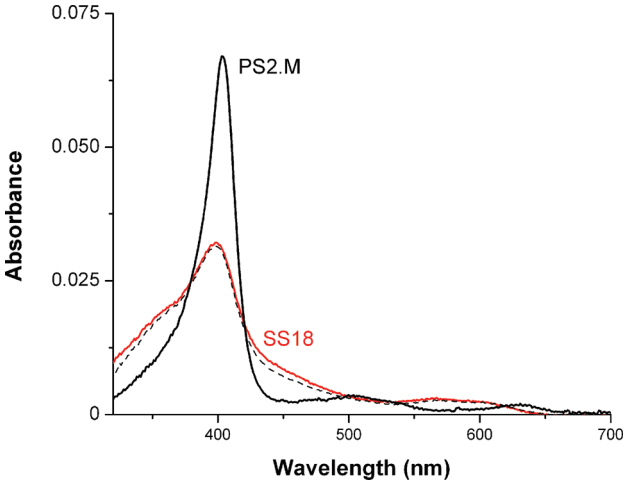

Figure 2. UV−vis absorption spectrum of the PS2.M·heme complex (continuous black line), compared to the spectra of soluble, monomeric Fe(III) heme in the absence of DNA (dotted black line) and in the presence of a nonbinding DNA oligonucleotide, SS18 (continuous red line). That the soluble, monomeric heme studied here is indeed that, and not a nonspecific aggregate, has been carefully monitored and reported in our earlier work.[9]

M with submicromolar affinity.[9] Figure 2 shows that Fe(III) heme, when fully complexed with PS2.M, reveals a characteristic hyperchromicity of its Soret absorption band as well as changes in its visible spectrum (relative to soluble, monomeric Fe(III) heme[9] in the absence of DNA or mixed with a nonbinding single-stranded DNA, SS18). Travascio et al. measured the rate of peroxidation of a chromogenic substrate, ABTS, to a radical cation product, $ABTS^{\bullet+}$, by PS2.M·Fe(III) heme and found it to be ~50-fold faster relative to the two controls described above.[9,11] In essence, the guanine-rich oligonucleotide, PS2.M, folds to a guanine quadruplex and functions as an apoenzyme for the heme cofactor. Both RNA and DNA are known to fold to G-quadruplexes;[12] remarkably, the RNA counterpart of PS2.M (rPS2.M) shows Fe(III) heme binding and peroxidative activities comparable to those of PS2.M.[11] Recently, it has been shown that the above two properties are shared by most G-quadruplexes, whether DNA or RNA, including those putatively formed in vivo by chromosomal telomeres, gene promoters, and other G-rich genomic elements and transcripts.[13,14]

This remarkable peroxidase activity of the PS2.M·Fe(III) heme complex, and of numerous sequence variants of PS2.M complexed with heme, has since found a versatile practical utility. Applications include chemical sensing using colorimetry,[15−18] fluorescence,[19] electrochemistry,[20] and immunoblotting.[21] Other applications include bioelectronics,[22] the construction of a molecular machine,[23] use as an electrocatalyst,[24] and use in cancer immunohistology.[25]

In this paper, we report that the above DNA and RNA G-quadruplexes, when complexed with heme, show an additional, robust, catalytic activity—namely, oxygen atom transfer from hydrogen peroxide to a variety of substrates, including thioanisoles, indole, and styrene. These oxygen transfer reactions constitute 2-electron oxidations, in marked contrast to the 1-electron peroxidations described above.

RESULTS

Oxygen Transfer to Thioanisole and to Substituted Thioanisoles. We were interested to know whether PS2.M·heme was capable of any of the other known activities of heme proteins—for instance, catalysis of the mechanistically more complex 2-electron oxidations. We chose thioanisole, a widely used test substrate for oxygen transfer reactions.[26−35] PS2.M·heme was activated (in the presence of 1.0 μM Fe(III) heme, 3.0 μM DNA, and 0.2 mM thioanisole) with 1 mM H_2O_2, under solution conditions optimized earlier for PS2.M·heme's peroxidase activity.[9] Analysis over a 30 min period, at 21 °C, showed the rapid appearance of the thioanisole sulfoxide (TSO) product in the PS2.M·heme solution but not in a control solution containing Fe(III) heme and the non-G-quadruplex-forming SS18 oligonucleotide. Figure 3a plots the time courses for the two solutions. The SS18/Fe(III) heme solution generates TSO at extremely low levels, whereas the calculated turnover rate of 3.5 s^{-1} for PS2.M·heme (initial rate of 3.5 μM s^{-1} catalyzed by 1.0 μM PS2.M·heme) compares favorably with those of classical peroxidases:[35] myeloperoxidase, 4 s^{-1};[35] lactoperoxidase, 0.1 s^{-1};[32] HRP, 0.05 s^{-1}.[31]

To investigate whether the oxygen transferred to thioanisole by PS2.M·heme in fact originates from H_2O_2, we carried out an experiment using ^{18}O-labeled H_2O_2, which contained 90 atom % ^{18}O. Figure S1 (Supporting Information) shows that 89% of the resulting TSO product was labeled with ^{18}O (given the 90 atom % ^{18}O in the $H_2{}^{18}O_2$, the TSO oxygen was derived quantitatively from H_2O_2). The products of heme enzymes known to use the oxygen rebound mechanism generally show <100% incorporation of oxygen from H_2O_2, since a proportion of the radical intermediate diffuses away from the heme and receives oxygen from sources other than H_2O_2.[34,35] However, our data with PS2.M·heme suggest that thioanisole, whether oxygenated in one step or two, must interact more than transiently with the DNAzyme's catalytic core. To probe the nature of PS2.M·heme's active site, we checked for enantioselectivity in its oxygen transfer to thioanisole. Most protein peroxidases show a marked preference for generating one or the other enantiomer of TSO (lactoperoxidase and myeloperoxidase favor the (*R*)-sulfoxide, while HRP favors the (*S*)-sulfoxide[35]). Analysis of the PS2.M·heme-generated TSO on a chiral HPLC column revealed that a racemic mixture was produced (Figure S2, Supporting

dx.doi.org/10.1021/ja108571a |J. Am. Chem. Soc. XXXX, XXX, 000–000

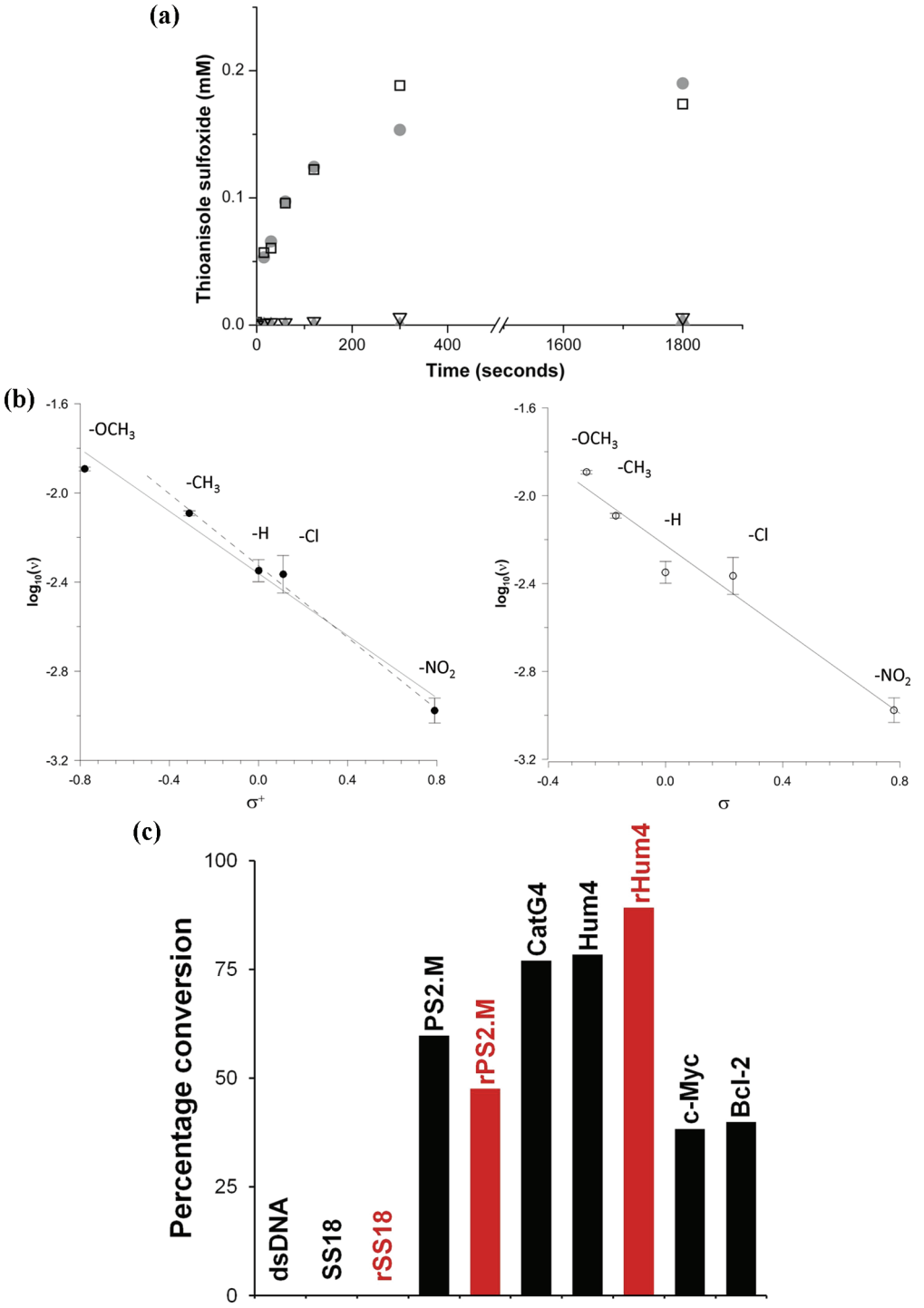

Figure 3. Studies on catalysis of oxygen transfer to thioanisole substrates. (a) Time courses for the generation of thioanisole sulfoxide from incubations of 0.2 mM thioanisole, at 21 °C, in oxidation buffer (40 mM HEPES−NH_4OH, pH 8.0, 20 mM KCl, 0.05% Triton X-100, 3% DMF) in the presence of 1 μM Fe(III) heme, 1 mM H_2O_2, and 3 μM DNA (PS2.M, ●, □; SS18, ▼, △). Two sets of independent measurements are shown. (b) Hammett plots for oxidation rates of various para-substituted thioanisoles. Log ν (where ν = initial rate of oxidation) is plotted against the substituent constants σ^+ (left panel) and σ (right panel). The data shown are the average of duplicate determinations, and the errors shown are the $N - 1$ standard deviations rather than the differences from the average. The uninterrupted line in either plot shows the best fit to all five data points. The stippled line in the σ^+ plot (left panel) shows the best fit for four data points, excluding that for *p*-methoxythioanisole. (c) Histogram showing the conversion (%) of thioanisole to thioanisole sulfoxide after 2 min of incubation in the presence of different DNA and RNA oligonucleotides, as well as a double-stranded DNA control (all sequences shown in Table 1). CatG4 has a slightly modified sequence but the same heme-binding properties as PS2.M.[60] Hum4 represents a four-repeat human telomeric DNA sequence, rHum4 represents an RNA version of Hum4, and c-Myc and Bcl-2 represent single-stranded G-rich DNAs from the respective oncogene promoters (12). The reaction conditions are the same as those for (a) (with the exception that the Hum4 and rHum4 solutions contained 120 μM DNA/RNA to ensure >90% binding of the heme to the DNA/RNA). The SS18 and dsDNA controls were tried with both 3 and 120 μM DNA, and no difference was found in the outcome.

dx.doi.org/10.1021/ja108571a |*J. Am. Chem. Soc.* XXXX, XXX, 000–000

Information). Klibanov and colleagues had earlier reported that PS2.M·heme lacks stereospecificity in its peroxidase activity;[36] it is interesting to note that a lack of stereoselectivity is also a feature of its catalysis of the more complex oxygen transfer reaction.

To probe this mechanism further, a Hammett analysis was carried out using para-substituted thioanisoles with electron-donating (methyl and methoxy) and -withdrawing (nitro and chloro) functionalities. The log of the initial oxidation rate (ν) was plotted against a substituent constant—either σ, which is based on an equilibrium ionization process, or σ^+, which is based on the rates for a carbenium ion forming reaction.[37] Figure 3b shows the two plots (σ^+, left, and σ, right), where correlations with σ^+ and σ are expected for mechanisms involving a two-step, oxygen rebound mechanism (formation of a sulfenium radical cation intermediate) or a one-step, direct oxygen transfer reaction, respectively. log ν values were found to correlate with the electron-donating power of the substituent ($\rho = -0.70 \pm 0.07$ in the σ^+ plot and -0.96 ± 0.12 in the σ plot), and both of these are consistent with a buildup of positive charge in the oxidation transition state. Also, shown in Figure 3b, left (drawn as a stippled line), is the fit that excludes the most electron donating substituent ($\rho = -0.81 \pm 0.05$). However, the difference in correlation coefficients among these three fits, which have R^2 values of 0.992 (stippled line σ^+), 0.973 (σ^+), and 0.958 (σ), is not significant enough, given the differences between the processes used to define σ and σ^+ and the current oxidation reaction, to permit a definitive mechanistic conclusion to be made.

A comparable analysis with the protein enzymes HRP and CPO has shown divergent results.[38] HRP showed a poor correlation of log ν with both σ and σ^+, suggesting that there were dominating steric constraints imposed by its active site. CPO, however, like PS2.M, showed a better correlation of log ν with σ^+ than with σ, suggesting that its catalysis followed the oxygen rebound mechanism.[38]

Finally, we investigated whether TSO formation could be catalyzed by RNA (rPS2.M and the human telomeric sequence, rHum) as well as by DNA other than PS2.M. Figure 3c shows that all of the G-quadruplex-forming RNA and DNA sequences tested (including Bcl-2 and c-Myc, sequences from human oncogene promoters) were catalytic, while the single-stranded DNA (SS18) and RNA (rSS18) as well as double-stranded DNA (dsDNA) controls were not. Oxygen transfer to thioether substrates can thus legitimately be added to the growing list of catalytic activities of both RNA and DNA.

Oxygen Transfer to Indole Yields Numerous Products. To investigate the versatility of oxygen transfer reactions catalyzed by RNA− and DNA−heme ("nucleoheme") complexes, indole was chosen as a second test substrate. The cytochrome P450s have been shown to oxygenate indole to a number of different products, including the dyes indigo and indirubin.[31] By contrast, scant literature exists on indole oxygenation by classical peroxidases: HRP is reported to be poorly active and to give uncertain products.[39] The nonclassical peroxidase, CPO, by contrast, actively generates a single oxygenation product, 2-oxindole.[39]

Solutions of 1 mM indole were made up to 10 μM Fe(III) heme and a 25 μM concentration of either PS2.M or SS18 and were activated with 1 mM H_2O_2. Figure 4a shows that a rich mixture of oxidized products, similar to those generated by cytochrome P450s,[40] appears from the PS2.M·heme solution in as little as 5 min. The SS18/heme control, by contrast, shows only traces of some of the same products. The major products identified (Table S1, Supporting Information) include isatin

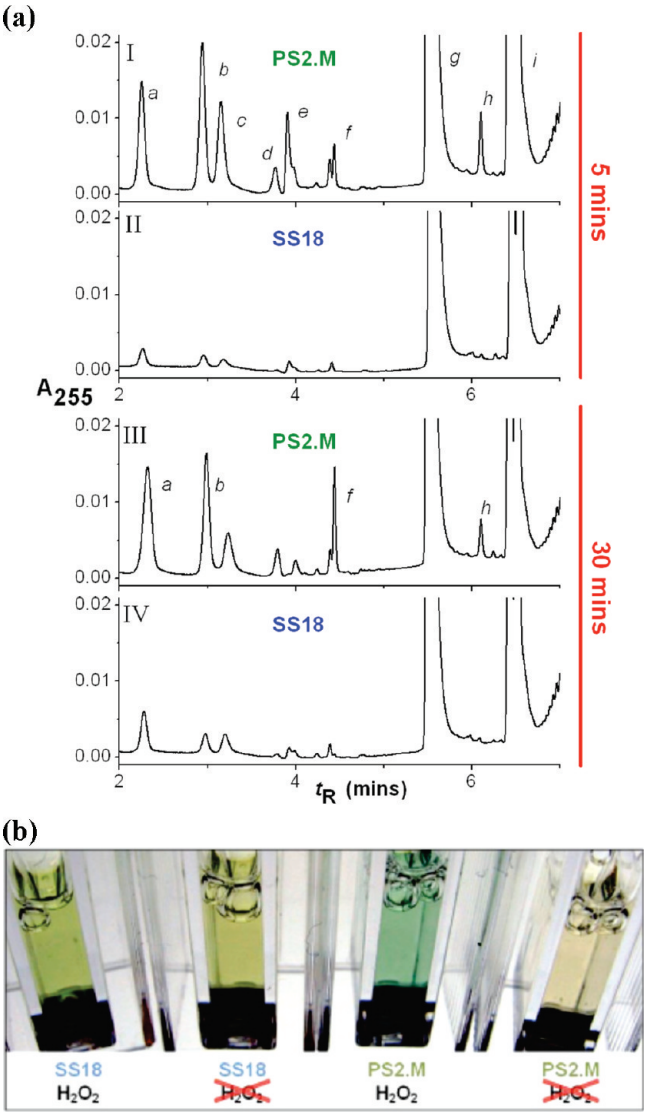

Figure 4. Catalyzed oxygen transfer to indole. (a) HPLC traces of indole oxidation products formed in incubations of 1 mM indole in I-oxidation buffer (40 mM HEPES−NH_4OH, pH 8.0, 20 mM KCl, 0.05% Triton X-100, 1% DMF), at 21 °C, in the presence of 10 μM Fe(III) heme, 1 mM H_2O_2, and 25 μM DNA (PS2.M or SS18). Incubation traces of 5 min (upper) and 30 min (lower) are shown. The major peaks, labeled *a*−*i*, were identified using LC−MS and by comparison with pure standards, as follows: *a*, isatin; *b*, 2-oxindole; *c* and *f* had the same molecular mass as indigo and indirubin (262 Da), but had absorption spectra that were distinct from those of indirubin and indigo; *d*, unidentified product with the same molecular mass as isatin (147 Da); *e*, unidentified product; *g*, unreacted indole; *h*, indigo; *i*, benzophenone (added internal standard). (b) Appearance of an indigo blue color after a 1 min incubation of 2 mM indole in the presence of 10 μM Fe(III) heme, 1 mM H_2O_2, and 25 μM PS2.M (third cuvette from left). Controls containing SS18 instead of PS2.M, and those where no H_2O_2 was added, are shown as indicated. It is notable also that the PS2.M incubation without added H_2O_2 (far right) has the red color characteristic of the PS2.M·heme complex, relative to the yellow color of unbound Fe(III) heme (second from the left).

(*a* in Figure 4a), 2-oxindole (*b*), indigo (*g*), and indigoid products (*c* and *f*, each with the mass of indigo and indirubin, 262 Da), whose absorption spectra differ from those of indirubin and indigo. At 30 min of incubation, the relative yield of the products was

dx.doi.org/10.1021/ja108571a |J. Am. Chem. Soc. XXXX, XXX, 000–000

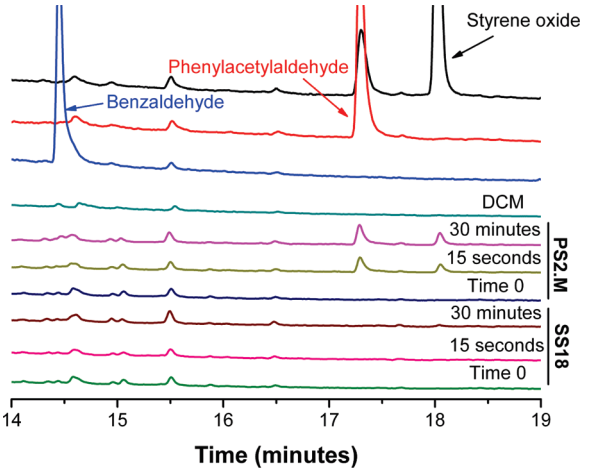

Figure 5. Catalyzed oxygen transfer to styrene. Gas chromatographs showing the production of phenylacetaldehyde and styrene oxide from incubations of PS2.M·heme with styrene and hydrogen peroxide and the absence of formation of these products, under the same conditions, from a solution in which the DNA oligomer SS18 substitutes for PS2.M. A trace of benzaldehyde can be detected in the 30 min incubation of PS2.M·heme with styrene and hydrogen peroxide. Chromatographs of the pure compounds phenylacetaldehyde, styrene oxide, benzaldehyde, and dicholoromethane are shown above the products from the PS2.M·heme and SS18/heme incubations. It should be noted that the styrene oxide standard contains a small amount of phenylacetaldehyde as a contaminant.

different, possibly, in part, due to air oxidation of the initial products. Figure 4b shows that, within 1 min, the incubation of indole with PS2.M·heme and H_2O_2 develops a blue indigo color. That oxygen transfer to indole is a general property of a variety of DNA and RNA nucleoheme complexes is summarized in Figure S3, Supporting Information.

Styrene Oxidation Yields Styrene Oxide and Phenylacetaldehyde. The epoxidation of alkenes has been described as the "holy grail in catalytic oxidation".[35] Epoxidation is a relatively challenging oxidation by virtue of the high oxidation potential involved.[41] A classical peroxidase, such as HRP, catalyzes epoxidation of styrene very poorly;[42,43] P450 monooxygenases and nonclassical peroxidases (such as CPO), however, typically show more efficient catalysis of styrene epoxidation (CPO has k_{cat} values of 0.1−4.0 s^{-1},[44] and the P450 enzymes show comparable values[35]). When styrene is the substrate, in addition to the expected styrene oxide product, phenylacetaldehyde (PAA; formed by a hydrogen rearrangement[42,43]) is often produced; furthermore, some enzymes generate benzaldehyde using an unknown mechanism.[29] Figure 5 shows that PS2.M·heme catalyzes the formation of two products which, upon comparison with standards, can be identified as styrene oxide and PAA. A very low amount of benzaldehyde (relative to yields of styrene oxide and PAA) could also be detected by GC−MS in the 30 min PS2.M·heme incubation. Initial rates are measured to be, for PAA, ≥1.7 $\mu M\ s^{-1}$ and, for SO, ≥0.4 $\mu M\ s^{-1}$ (corresponding to turnover numbers of ∼1.7 and ∼0.4 s^{-1}, respectively). As with thioanisole, PS2.M·heme appears to be a superior catalyst for styrene oxidation relative to the classical peroxidases. Curiously, the reaction of H_2O_2 with styrene in this system proceeds only for a short time (∼1 min), owing to the likely destruction of PS2.M·heme. Similar observations have also ben made with a number of heme enzymes.[45]

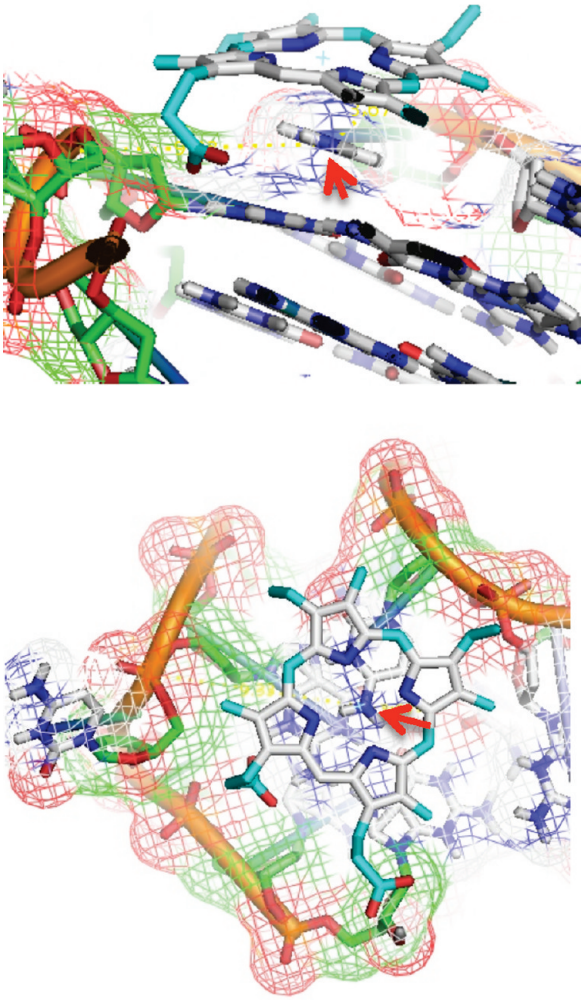

Figure 6. Structure of Fe(III) heme docked, using the Autodock program, upon the G-quadruplex formed by the Bcl-2 DNA oligomer, shown as a top view (above) and a side view (below). The red arrow in each case indicates the position of the exocyclic amino group of the C6 residue of the G-quadruplex. The distance from this amino group to the iron at the center of the heme (unshown) is ∼2.74 Å.

Does the oxygen within styrene oxide generated by PS2.M·heme originate from the latter's ferryl oxygen (which is, in turn, generated from the H_2O_2)? Among heme enzymes, CPO incorporates ^{18}O from $H_2{}^{18}O_2$ quantitatively into styrene oxide.[45] However, only 79% of the styrene oxide generated by HRP originates from H_2O_2;[42] the rest originates, presumably, from dioxygen. Wild-type HRP is able to use H_2O_2 and dioxygen together to co-oxidize phenols and styrene (here, the oxygen of styrene oxide is derived purely from the dioxygen[46]). The data shown in Figure S4, Supporting Information, indicate that 73% of the oxygen of styrene oxide (corrected for the ^{18}O purity of the $H_2{}^{18}O_2$) catalyzed by PS2.M·heme is derived from $H_2{}^{18}O_2$. Thus, as observed with the thioanisole substrate, oxygen transfer to styrene substrate proceeds primarily from the activated ferryl species within PS2.M·heme.

DISCUSSION

How do G-quadruplex nucleoheme complexes catalyze oxygen transfer? Oxidative, heme-containing, protein enzymes realize

dx.doi.org/10.1021/ja108571a |J. Am. Chem. Soc. XXXX, XXX, 000–000

Table 1. DNA and RNA Sequences[a]

name	sequence
dsDNA	5′-TTT AGT CGA CCT CGC CCC CGC TGC CAT AGT GAC ACA-3′
	3′-AAA TCA GCT GGA GCG GGG GCG ACG GTA TCA CTG TGT-5′
SS18	5′-AAT ACG ACT CAC TAT ACT-3′
rSS18	5′-AAU ACG ACU CAC UAU ACU-3′
PS2.M	5′-GTG GGT AGG GCG GGT TGG-3′
rPS2.M	5′-GUG GGU AGG GCG GGU UGG-3′
CatG4	5′-TGG GTA GGG CGG GTT GGG AAA-3′
Hum4	5′-TTA GGG TTA GGG TTA GGG TTA GGG-3′
rHum4	5′-UUA GGG UUA GGG UUA GGG UUA GGG-3′
c-Myc	5′-TGA GGG TGG GGA GGG TGG GGA A-3′
Bcl-2	5′-GGG CGC GGG AGG AAG GGG GCG GG-3′

[a] RNA sequences have an "r" prefix.

their catalytic properties by supplying a key axial ligand to the heme iron, which controls the iron's reactivity. Specificity is realized by allowing differential substrate access to the oxoiron moiety of compound I.[47] In an earlier study on PS2.M·heme, we found evidence that the DNA provides axial coordination of the heme, probably using a nucleobase.[48] This has not been elaborated on, however, since no high-resolution structure exists to date for PS2.M·heme. However, high-resolution NMR structures do exist for the c-Myc[49] and Bcl-2 G-quadruplexes.[50] We have shown, above, that these quadruplexes bind heme and actively catalyze oxygen transfer (Figure 3c). Phan et al. reported an NMR structure of the c-Myc G-quadruplex bound to a cationic (and unmetalated) porphyrin, TMPyP4, and found it to stack, somewhat asymmetrically, atop a guanine quartet.[49] We were uncertain to what degree it might be possible to extrapolate this result to the binding of heme to a G-quadruplex. We therefore performed flexible docking, using the software Autodock, to identify likely heme-binding site(s) on the NMR-derived structure of the Bcl-2 quadruplex. Figure 6 shows the common heme location for all of the lowest energy docked structures obtained. The heme stacks upon a loop cystosine, C6, which in turn stacks upon the G-quartets. Interestingly, the exocyclic amine of C6 lies close to and axial to the heme iron, at a distance of ∼2.74 Å (in heme enzymes, the iron to axial ligand distances are in the 2.1−2.4 Å range[51]). Our earlier EPR[48] and UV−vis spectroscopic[9] data had indicated a 6-coordinate, high-spin, ferric iron in PS2.M·heme (with a likely fifth coordination from the DNA and the sixth from water). The lack of a structured environment on the distal side of the heme (away from the G-quadruplex) is undoubtedly linked to the lack of enantioselectivity of these catalytic complexes. Purely 1-electron (peroxidase) reactions have been proposed to require only a collision of the substrate with the edge of heme compound I;[47] by contrast, oxygen transfer (whether proceeding in one or two steps) necessarily requires the persistent localization of the substrate close to the heme's ferryl oxygen. If indeed oxygen transfer catalyzed by nucleoheme complexes proceeds in two steps, those steps must be tightly coupled. For the second oxidation step, the thioanisole and indole radical cations might interact with the DNA/RNA-bound heme via $\pi-\pi$ as well as $\pi-$cation interactions.[52]

Like other enzymatic cofactors, heme is likely a primordial compound—one that could have participated in the postulated RNA world.[53] Our evidence that nucleoheme complexes can recapitulate more than one catalytic function (i.e., both 1- and 2-electron oxidations) of contemporary heme enzymes elicits the following question: what other properties of heme proteins are also realizable by nucleoheme complexes? We are currently investigating this question.

The porphyrins that do bind G-quadruplexes have been found to stabilize the G-quadruplex fold.[54] It is likely, even in the absence of direct evidence, that heme binding correspondingly stabilizes the RNA and DNA folds within nucleoheme complexes. Riboswitches[54] are ligand-binding RNA motifs that serve as feedback modules in the control of various metabolic pathways, particularly the biosynthetic pathways for nucleobases and enzymatic cofactors. It may be instructive to investigate (a) whether RNA transcripts coding for different enzymes in the heme biosynthetic pathways fold to form G-quadruplexes and (b) whether the translation of these transcripts is modulated by the binding of heme.

The simple RNA and DNA quadruplex folds we have explored here likely generate relatively "open" active sites upon heme binding. However, more complex RNA and DNA folds that nevertheless incorporate heme-binding sites may endow both substrate and reaction specificity to nucleoheme complexes to levels found in protein heme enzymes. This is a subject under active investigation in our laboratory. Cytochrome P450 enzymes are widely regarded as promising catalysts for the stereo- and regioselective synthesis of valuable chemicals on an industrial scale.[35] It is conceivable that nucleoheme complexes may find a comparable utility, given that they are likely to offer excellent price as well as chemical stability advantages over recombinant proteins.

The formation of G-quadruplex structures in vivo is a subject of great current interest: chromosomal telomeres within ciliate macronuclei have been shown convincingly to form G-quadruplexes,[56] a DNA quadruplex has been implicated in the pilin antigenic variation in *Neisseria gonorrheae*,[57] and a variety of mammalian DNA and RNA sequences, from oncogene promoters to telomeres, have also been postulated to form quadruplexes in vivo.[11] On the basis of our data, explorations of such structures should take cognizance of their potential for oxidative catalysis in vivo. For instance, it has recently been proposed that, in Alzheimer's disease patients, amyloid-β peptide, the toxic agent of the disease, both sequesters and binds heme, giving rise not only to a functional heme deficiency but to a surprisingly effective and potentially toxic intracellular peroxidase activity.[58] In a corresponding manner, it is possible to conceptualize disease states in which an overabundance of guanine-rich RNA transcripts accumulate in the cell. Such transcripts may then sequester away

dx.doi.org/10.1021/ja108571a |*J. Am. Chem. Soc.* XXXX, XXX, 000–000

heme required for optimal cellular function, as well as catalyze 1- and 2-electron oxidative reactions that are detrimental to the cell.

Given the ease of oxidation of indole and its derivatives by nucleoheme complexes, it is also interesting to note that oxidation of externally administered indoleacetic acid (IAA) by peroxidases has shown promise as an anticancer therapeutic strategy.[59] It will be intriguing to see if nucleoheme complexes can be brought to participate in such a strategy and perhaps offer advantages over the use of potentially immunogenic protein peroxidases.

EXPERIMENTAL SECTION

Materials. All DNA was purchased from Integrated DNA Technologies, Inc. All RNA was purchased from University Core DNA Services (University of Calgary). The sequences of all DNAs and RNAs are given in Table 1. All nucleic acids were purified by preparative gel electrophoresis, eluted, ethanol precipitated, and then stored dissolved in TE buffer [10 mM Tris, pH 7.5, and 0.1 mM ethylenediaminetetraacetate (EDTA)]. All chemicals were purchased from Sigma-Aldrich, unless specified otherwise. Fe(III) heme (hemin) was purchased from Porphyrin Products (Logan, UT). ^{18}O-Hydrogen peroxide was purchased from Icon Isotopes (Summit, NJ).

UV−Vis Spectroscopy of Fe(III) Heme and Nucleoheme Complexes. A 1 mL solution containing 1 μM PS2.M or SS18 and 0.5 μM Fe(III) heme in spectroscopy buffer [50 mM MES (2-(*N*-morpholino)ethanesulfonic acid), pH 6.2, 100 mM Tris−acetate, 20 mM potassium acetate, 0.05% Triton X-100, 1% DMSO] was incubated for 30 min at 21 °C to permit DNA−heme interactions, where possible. Spectra taken in oxidation buffer and in I-oxidation buffer (see below) give the same results. The UV−vis spectra of PS2.M with Fe(III) heme, SS18 with Fe(III) heme, and Fe(III) heme alone were obtained using a Cary 300 Bio UV−vis spectrophotomer. Any background from buffer alone was subtracted from the sample spectra.

Time Course Measurements on Thioanisole Sulfoxidation. A 32 μL volume of a 100 μM DNA stock in TE buffer and 10 μL of 100 μM Fe(III) heme in DMF were added to 500 μL of a 2× buffer (80 mM HEPES−NH_4OH, pH 8.0, 40 mM KCl, 0.1% Triton X-100, and 2% DMF) in a 1.5 mL glass vial. ddH_2O was added to make the volume 980 μL. The solution was incubated for 5 min at 21 °C to allow for DNA−heme interactions. A 10 μL volume of 20 mM thioanisole in DMF was added to the solution, and the resulting solution was vortexed to mix. Prior to the start of the oxidation reaction, a 99 μL aliquot was set aside for time 0 (and was treated as described below). The reaction was initiated by the addition of 9 μL of 100 mM H_2O_2. The resulting 900 μL volume containing 0.2 mM thioanisole, 1 μM Fe(III) heme, 3 μM DNA, and 1 mM H_2O_2 in oxidation buffer (40 mM HEPES−NH_4OH, pH 8.0, 20 mM KCl, 0.05% Triton X-100, 3% DMF) was incubated at room temperature. Aliquots of 95 μL of the reaction mixture were removed at time 0 and 15 s, 30 s, 1 min, 2 min, 5 min, and 30 min after initiation of the reaction. A 5 μL volume of 1 mM benzophenone was added as an internal standard to each aliquot prior to addition of 200 μL of CH_2Cl_2, both to quench the reaction and to extract the contents of the aqueous reaction mixture, which was analyzed using HPLC (see the Supporting Information).

Para-Substituted Thioanisole Sulfoxidations. The procedure was substantially as described above. See the Supporting Information for the details of analysis.

Hammett Analysis, Analysis of the Source of the Oxygen in the TSO Product, Analysis of the Stereochemistry of Thioanisole Sulfoxidation, and TSO Formation by Different DNAs and RNAs. See the Supporting Information.

Indole Oxidation Reactions. Reactions were carried out in I-oxidation buffer (40 mM HEPES−NH_4OH, pH 8.0, 20 mM KCl, 0.05% Triton X-100, and 1% DMF), at 21 °C, containing 1 mM H_2O_2, 1 mM indole, 10 μM Fe(III) heme, and 25 μM DNA/RNA. The lower DMF content of this buffer, relative to that used for thioanisole oxidation, is in response to the higher aqeuous solubility of indole. At specified times, 95 μL of each reaction mixture was supplemented with 5 μL of 1 mM benzophenone (internal standard) and then immediately placed at −80 °C to stop the reactions. Samples were later thawed and analyzed using HPLC. Details of the HPLC runs are given in the Supporting Information.

Indigo Cuvette Image Protocol. Each reaction was carried out on a 500 μL scale. Reactions consisted of indole (2 mM), DNA (25 μM), and Fe(III) heme (10 μM) in I-oxidation buffer. A 5 μL volume of hydrogen peroxide (100 mM) was added to specific cuvettes, and not to other cuvettes, and the contents were mixed. After approximately 5 min, the blue color reached saturation; the cuvettes were then set up on a white light box for photography. The brightness and contrast for the images were later optimized.

Styrene Oxidation. See the Supporting Information.

Heme Docking upon the Bcl-2 DNA G-Quadruplex. See the Supporting Information.

ASSOCIATED CONTENT

Supporting Information. Details of experimental protocols and data on the enantioselectivity and H_2O_2 utilization properties of nucleoheme complexes for oxygen transfer reactions. This material is available free of charge via the Internet at http://pubs.acs.org.

AUTHOR INFORMATION

Corresponding Author
sen@sfu.ca

ACKNOWLEDGMENT

We are grateful to Erika Plettner, Peter Unrau, and the laboratories of Robert Young, Gerhard Gries, and Robert Britton for their advice and for access to their equipment. We also appreciate the help of the technical staff of the Simon Fraser University Chemistry Department. This work was supported by a grant to D.S. from the Natural Sciences and Engineering Research Council of Canada (NSERC). D.S. is a fellow of the Canadian Institute for Advanced Research (CIFAR).

REFERENCES

(1) Doudna, J. A.; Cech, T. R. *Nature* **2002**, *418*, 222.
(2) Höbartner, C.; Silverman, S. K. *Biopolymers* **2007**, *87*, 279.
(3) Gilbert, W. *Nature* **1986**, *319*, 618.
(4) White, H. B., 3rd. *J. Mol. Evol.* **1976**, *7*, 101.
(5) Benner, S. A.; Ellington, A. D.; Tauer, A. *Proc. Natl. Acad. Sci. U.S.A.* **1989**, *86*, 7054.
(6) Eddy, S. R. *Nat. Rev. Genet.* **2001**, *2*, 919.
(7) Marnett, L. J.; Kennedy, T. A. In *Cytochrome P450, Structure, Mechanism, and Biochemistry*; Ortiz de Montellano, P. R., Ed.; Plenum Press: New York, 1995; pp 49−80.
(8) Bröring, M. . In *Iron Catalysis in Organic Chemistry*; Plietker, B., Ed.; Wiley-VCH Verlag GmbH Co. KGaA: Weinheim, Germany, 2008; pp 48−72.
(9) Travascio, P.; Li, Y.; Sen, D. *Chem. Biol.* **1998**, *5*, 505.
(10) Li, Y.; Sen, D. *Nat. Struct. Biol.* **1996**, *3*, 743.
(11) Travascio, P.; Bennet, A. J.; Wang, D. Y.; Sen, D. *Chem. Biol.* **1999**, *6*, 779.
(12) Lipps, H. J.; Rhodes., D. *Trends Cell. Biol.* **2009**, *19*, 414.

(13) Kong, D. M.; Yang, W.; Wu, J.; Li, C. X.; Shen, H. X. *Analyst* **2010**, *135*, 545.
(14) Cheng, X.; Liu, X.; Bing, T.; Cao, Z.; Shangguan, D. *Biochemistry* **2009**, *48*, 7817.
(15) Kong, D. M.; Wu, J.; Ma, Y. E.; Shen, H. X. *Analyst* **2008**, *133*, 1158.
(16) Li, T.; Wang, E.; Dong, S. *Chem. Commun. (Cambridge)* **2008**, *31*, 3654.
(17) Deng, M.; Zhang, D.; Zhou, Y.; Zhou, X. *J. Am. Chem. Soc.* **2008**, *130*, 13095.
(18) Nakayama, S.; Sintim, H. O. *J. Am. Chem. Soc.* **2009**, *131*, 10320.
(19) Nakayama, S.; Sintim, H. O. *Mol. Biosyst.* **2010**, *6*, 95.
(20) Zhang, K.; Zhu, X.; Wang, J.; Xu, L.; Li, G. *Anal. Chem.* **2010**, *82*, 3207.
(21) Li, J.; Yao, J.; Zhong, W. *Chem. Commun. (Cambridge)* **2009**, *33*, 4962.
(22) Willner, I.; Willner, B.; Katz, E. *Bioelectrochemistry* **2007**, *70*, 2.
(23) Weizmann, Y.; Cheglakov, Z.; Willner, I. *J. Am. Chem. Soc.* **2008**, *130*, 17224.
(24) Pelossof, G.; Tel-Vered, R.; Elbaz, J.; Willner, I. *Anal. Chem.* **2010**, *82*, 4396.
(25) Thirstrup, D.; Baird, G. S. *Anal. Chem.* **2010**, *82*, 2498.
(26) Doerge, D. R. *Arch. Biochem. Biophys.* **1986**, *244*, 678.
(27) Fruetel, J. A.; Chang, Y. T.; Collins, J.; Loew, G.; Ortiz de Montellano, P. R. *J. Am. Chem. Soc.* **1994**, *116*, 11643.
(28) Adam, W.; Mock-Knoblauch, C.; Saha-Möller, C. R. *J. Org. Chem.* **1999**, *64*, 4834.
(29) Savenkova, M. I.; Newmyer, S. L.; Ortiz de Montellano, P. R. *J. Biol. Chem.* **1996**, *271*, 24598.
(30) Ozaki, S.; Yang, H.-J.; Matsui, T.; Goto, Y.; Watanabe, Y. *Tetrahedron: Asymmetry* **1999**, *10*, 183.
(31) Tuynman, A.; Vink, M. K. S.; Dekker, H. L.; Schoemaker, H. E.; Wever, R. *Eur. J. Biochem.* **1998**, *258*, 906.
(32) Tuynman, A.; Schoemaker, H. E.; Wever, R. *Monatsh. Chem.* **2000**, *131*, 687.
(33) Harris, R. Z.; Newmyer, S. L.; Ortiz de Montellano, P. R. *J. Biol. Chem.* **1993**, *268*, 1637.
(34) Doerge, D. R.; Cooray, N. M.; Brewster, M. E. *Biochemistry* **1991**, *30*, 8960.
(35) van Rantwijk, F.; Sheldon, R. A. *Curr. Opin. Biotechnol.* **2000**, *11*, 554.
(36) Rojas, A. M.; Gonzalez, P. A.; Antipov, E.; Klibanov, A. M. *Biotechnol. Lett.* **2007**, *29*, 227.
(37) Isaacs, N. *Physical Organic Chemistry*; Prentice Hall: Upper Saddle River, NJ, 1996; p 152.
(38) Kobayashi, S.; Nakano, M.; Kimura, T.; Schaap, A. P. *Biochemistry* **1987**, *26*, 5019.
(39) Corbett, M. D.; Chipko, B. R. *Biochem. J.* **1979**, *183*, 269.
(40) Gillam, E. M.; Notley, L. M.; Cai, H.; De Voss, J. J.; Guengerich, F. P. *Biochemistry* **2000**, *39*, 13817.
(41) Tuynman, A.; Spelberg, J. L.; Kooter, I. M.; Schoemaker, H. E.; Wever, R. *J. Biol. Chem.* **2000**, *275*, 3025.
(42) Ozaki, S.-i.; Ortiz de Montellano, P. R. *J. Am. Chem. Soc.* **1995**, *117*, 7056.
(43) Miller, V. P.; DePillis, Ferrer, J. C.; Mauk, A. G.; Ortiz de Montellano, P. R. *J. Biol. Chem.* **1992**, *267*, 8936.
(44) Yi, X.; Mroczko, M.; Manoj, K. M.; Wang, X.; Hager, L. P. *Proc. Natl. Acad. Sci. U.S.A.* **1999**, *96*, 12412.
(45) Ortiz de Montellano, P. R.; Choe, Y. S.; DePillis, G.; Catalano, C. E. *J. Biol. Chem.* **1987**, *262*, 11641.
(46) Ortiz de Montellano, P. R.; Grab, L. A. *Biochemistry* **1987**, *26*, 5310.
(47) Ator, M. A.; Ortiz de Montellano, P. R. *J. Biol. Chem.* **1987**, *262*, 1542.
(48) Travascio, P.; Witting, P. K.; Mauk, A. G.; Sen, D. *J. Am. Chem. Soc.* **2001**, *123*, 1337.
(49) Phan, A. T.; Kuryavyi, V.; Gaw, H. Y.; Patel, D. J. *Nat. Chem. Biol.* **2005**, *1*, 167.
(50) Dai, J.; Chen, D.; Jones, R. A.; Hurley, L. H.; Yang, D. *Nucleic Acids Res.* **2006**, *34*, 5133.
(51) Hersleth, H.-P.; Ryde, U.; Rydberg, P.; Görbitz, C. H.; Andersson, K. K. *J. Inorg. Biochem.* **2006**, *100*, 460.
(52) Gallivan, J. P.; Dougherty, D. A. *Proc. Natl. Acad. Sci. U.S.A.* **1999**, *96*, 9459.
(53) Yarus, M. *Annu. Rev. Genet.* **2002**, *36*, 125.
(54) Neidle, S.; Read, M. A. *Biopolymers* **2000−2001**, *56*, 195.
(55) Tucker, B. J.; Breaker, R. R. *Curr. Opin. Struct. Biol.* **2005**, *15*, 342.
(56) Paeschke, K.; Juranek, S.; Simonsson, T.; Hempel, A.; Rhodes, D.; Lipps, H. J. *Nat. Struct. Mol. Biol.* **2008**, *15*, 598.
(57) Cahoon, L. A.; Seifert, H. S. *Science* **2009**, *325*, 764.
(58) Atamna, H.; Boyle, K. *Proc. Natl. Acad. Sci. U.S.A.* **2006**, *103*, 3381.
(59) Wardman, P. *Curr. Pharm. Des.* **2002**, *8*, 1363.
(60) Elbaz, J.; Shlyahovsky, B.; Willner, I. A. *Chem. Commun.* **2008**, *13*, 1569.